# Breakdown of the Gouy−Chapman Model for Highly Charged Langmuir Monolayers: Counterion Size Effect

**Vladimir L. Shapovalov*,† and Gerald Brezesinski‡**

*N.N. Semenov Institute of Chemical Physics RAS, Kosygina 4, 119991 Moscow, Russia, and Max-Planck Institute of Colloids and Interfaces, D-14424 Potsdam, Germany*

*Received: November 23, 2005; In Final Form: March 24, 2006*

Deviations from the classic Gouy−Chapman (GC) model due to the finite size of hydrated counterions were tested for negatively charged Langmuir monolayers with different surface charge densities. Monolayers with the largest charge density (>0.6 C·m$^{-2}$) show an increase of the surface potential for a series of alkali metal cations from $Li^+$ to $Cs^+$ by 200−250 mV. The increase is similar for different monolayers and suggests that this effect is independent of the particular type of headgroup. The magnitude of variation is comparable with model estimations of the electrical double layer (EDL) potential implying that the deviation from the GC model is drastic. Deviations from the GC model rapidly vanish with decreasing monolayer charge density and become hardly observable below 0.3 C·m$^{-2}$. For monolayers with a high charge density on subphases containing different sized counterions, preferential participation of the smallest ions in the EDL should be favorable in terms of electrostatic free energy because of packing density limitations. This effect was demonstrated for behenyl sulfate (BS) monolayers (0.64 C·m$^{-2}$) with the X-ray reflectivity technique. For the $Cs^+$−$Li^+$ system, the fraction of $Cs^+$ in the EDL is 50−60% compared with only 10% of $Cs^+$ in the subphase. Providing high surface charge density, a small univalent $Cs^+$ is capable to compete even with a bulky divalent $Mg^{2+}$. For equal concentrations of $Cs^+$ and $Mg^{2+}$ in the subphase, the $Cs^+/Mg^{2+}$ ratio in EDL of BS monolayer is 1.3 to 2.0 (in contrast to 0.04, predicted by the GC model). All experimental results of this study are described in terms of packing density limitations for hydrated counterions in the EDL.

**Abbreviations:** EDL, electrical double layer; GC, Gouy−Chapman; BS, behenyl sulfate; AS, arachidyl sulfate; PFMA, perfluorinated myristic acid; DHDP, dihexadecyl phosphate; DOPG, dioleoylphosphatidylglycerol.

## Introduction

Electric fields and concentration profiles of ions in the vicinity of lipid membranes are the key factors for membrane protein function and, therefore, the existence of all living cells. To describe electric field and concentration profiles near a charged interface the classical Gouy−Chapman (GC) model of electrical double layer (EDL) is commonly used. However, basic assumptions of this model are not (strictly) applicable to the lipid−water interface: For example, the surface is not homogeneously charged, ions may penetrate it, and they are not infinitely small. Nevertheless, experimental data describing EDL near the lipid−water interface (ζ-potential for lipid vesicles, surface potential for charged Langmuir monolayers) are usually reported to be consistent with the GC model.

On the other hand, there are multiple reports of pronounced differences in the properties of charged monolayers,[1−6] micelles,[7,8] vesicles,[9] and dispersions[10,11] with different identically charged counterions. The so-called "counterion effect" is usually discussed in terms of the Hofmeister series for cations or anions.[11−15] On closer examination, at least some of such experimental observations are in opposition to the GC model. Indeed, if specific chemical interactions can be excluded (e.g. for alkali metal cations), the effect of counterions on the properties of a system which includes charged interfaces can result only from their effect on structure and energy of EDL. The last contradicts the GC model which predicts the same properties of EDL for any counterions of a given charge which are treated as idealized "point charges" (providing the same electrolyte concentration and surface charge density at the interface).

One of common arguments in favor of the GC model is the observation of a "theoretical slope" for semilogarithmic plots of the electric potential against electrolyte concentration in solution.[16−18] As a matter of fact, the "theoretical slope" of $kT/ze$ (where $k$ is the Boltzmann constant, $T$, the absolute temperature, $e$, the elementary charge, and $z$, the ion's valence) validates the Boltzmann law rather than the GC model. The Boltzmann expression for counterion concentration in the immediate vicinity of a charged plane $c_{cp}$,

$$c_{cp} = c_b \exp(-ze\varphi/kT)$$

(where $c_b$ is the concentration in bulk water and $\varphi$ is the electric potential of the plane), can be transformed to

$$\frac{\partial\varphi}{\partial(\ln c_b)} = \frac{kT}{ze}\left(1 - \frac{\partial(\ln c_{cp})}{\partial(\ln c_b)}\right)$$

Thus, the "theoretical slope" $kT/ze$ signifies that the second term in parentheses is negligible; i.e., the concentration of counterions near a charged plane is independent (or only weakly dependent) on the electrolyte concentration in bulk. Therefore, it is

* To whom correspondence should be addressed. Phone: +7 (495) 939-7345. Fax: +7 (495) 137-6130. E-mail: shapoval@center.chph.ras.ru.
† N.N. Semenov Institute of Chemical Physics RAS.
‡ Max-Planck Institute of Colloids and Interfaces.

10.1021/jp056801b CCC: $33.50 
Published on Web 05/04/2006

consistent with any model of EDL predicting such behavior. This fact is mentioned in fundamental monographs[19,20] but seldom recalled in later publications.

Furthermore, substitution of the electric potential value given by the Gouy−Chapman theory for the case of a 1−1-electrolyte,[20]

$$\phi = \frac{2kT}{e}\sinh^{(-1)}(\sigma/\sqrt{8\epsilon\epsilon_0 kT\cdot 10^3 N_a c_b})$$

into the Boltzmann equation yields physically irrelevant counterion concentrations[21] for reasonably high surface charge densities, $\sigma$.

Application of the GC model to a surface with charge density $\sigma = 0.6$ C·m$^{-2}$ (fully ionized condensed monolayers of single-chain amphiphiles) leads to a counterion concentration near the headgroup plane exceeding 100 M. This value strongly conflicts with packing density restrictions; the concentration of closely packed spherical particles with a radius of 3 Å, which is the typical size for a hydrated ion,[22] is only about 10 M.

The aim of this study is to check this weak point of the Gouy−Chapman model in application to highly charged Langmuir monolayers. The widely used Stern extension of the GC model, which eliminates the problem of physically irrelevant counterion concentrations, will be advisedly not considered for the following reasons. It operates with 2−4 parameters unobtainable in independent experiments, i.e., practically "adjustable parameters". The advantage of adjustable parameters is the possibility to describe a posteriori almost any experimental finding. The disadvantage is the poor capability to predict even basic experimental features a priori and therefore no real experimental verification of the model itself. Last, but not the least, the division of the EDL into the inner "Stern layer" and residual "diffuse" part (each driven by specific forces) is quite unnatural for lipid surfaces (in contrast to metal surfaces). In the absence of strong chemical interactions between lipid headgroups and ions, which are comparable with electrostatic forces by energy, there are no specific forces driving the formation of a Stern layer.

Obviously, strong specific chemical interactions responsible for the formation of a "true" Stern layer must also be observable unambiguously in bulk solution. Hence, the appropriate choice of charged amphiphiles and ions with no noticeable mutual complexing ability in bulk seems to be sufficient condition for the exclusion of a Stern layer from consideration.

To fulfill the conditions of high charge density and low complexing ability, Langmuir monolayers of long chain alkyl sulfates and a perfluorinated fatty acid were examined on subphases containing different alkali metal counterions. The headgroups of these monolayers are strongly acidic. It was shown that at pH 5−6 and salt concentrations above 1 mM they are completely deprotonated, i.e., negatively charged. Maximum packing density of all monolayers is close to 25 Å$^2$·molecule$^{-1}$. Therefore, their surface charge density reaches $e/(25\ \text{Å}^2) = 0.64$ C·m$^{-2}$. From chemical considerations, headgroups of these amphiphiles have no complexing ability with respect to alkali and alkaline earth metal cations in contrast to fatty acids and some phospholipids, which do complex alkaline earth and transition metal cations.

All the systems were studied with surface potential and surface pressure−area isotherm techniques. To determine the integral amount of counterions in the EDL, X-ray reflectivity experiments were performed using $Cs^+$ cations with a high X-ray contrast.

## Materials and Methods

Behenyl sulfate (BS) sodium salt was synthesized from behenyl alcohol and chlorosulfonic acid in carbon tetrachloride and then purified by multiple recrystallization from ethanol−toluene mixtures. Arachidyl sulfate (AS) sodium salt from Aldrich, dihexadecyl phosphate (DHDP) from Fluka, and dioleoylphosphatidylglycerol (DOPG) from Avanti Polar Lipids were used without additional purification. Purified perfluorinated myristic acid (PFMA) was kindly provided by Prof. O. Shibata (Kyushu University, Fukuoka, Japan).

Alkali metal chlorides and magnesium chloride (hexahydrate) were all of analytical grade and used without further purification. Subphase solutions were prepared from ultrapure water with 18.2 MΩ·cm specific resistance. Monolayers were spread from chloroform−methanol (4:1 w/w) solutions of amphiphiles with concentrations of 0.5−1 mM.

Surface potential experiments were performed using a 250 × 100 × 8 mm$^3$ Teflon trough with a single barrier (asymmetric compression) equipped with a homemade Kelvin probe sensor. The gold-plated electrode of 10 mm diameter vibrates at ca. 80 Hz, and an Ag/AgCl electrode is used as reference. Final surface potential data were referenced to the surface potential of a subphase without a spreaded monolayer in a usual way. Surface pressure isotherms were simultaneously recorded using a homemade electronic balance equipped with a 10 mm wide Wilhelmy plate made of filter paper. All experiments were performed at ambient temperature of 23−24 °C, without thermostating the subphase. For all subphase solutions the pH was between 5.5 and 6.5 (no buffer was used).

X-ray reflectivity (XR) experiments were performed on the liquid surface diffractometer installed at the synchrotron undulator beamline BW1 in HASYLAB, DESY (Hamburg, Germany).[23] The specular XR was measured as a function of the vertical incidence angle, $\alpha_i$, with the geometry, $\alpha_i = \alpha_f = \alpha$, where $\alpha_f$ is the vertical exit angle of the reflected X-rays, using a NaI scintillation detector. An X-ray wavelength of $\lambda = 1.304$ Å was used. XR data were collected as a function of the incidence angle, $\alpha_i$, varied in the range 0.05−5°, corresponding to a range 0.01−0.85 Å$^{-1}$ of the vertical scattering vector component $q_z = (4\pi/\lambda)\sin(\alpha)$. The background scattering from the subphase was measured at $2\theta_{hor} = 0.7°$ and subtracted from the signal measured at $2\theta_{hor} = 0$. Reflectivity data were fitted to total electron density profiles with the program Rfit2001 designed by O. V. Konovalov (ESRF, Grenoble, France).[24]

## Results and Discussion

Behenyl sulfate (BS) monolayers on subphases containing different alkali metal cations exhibit surface pressure−area isotherms (Figure 1a) which differ markedly. The relative shift of the isotherms for different counterions is in qualitative agreement with earlier results,[6] obtained for BS monolayers on subphases containing 0.1 mM of alkali metal chlorides. In the case of $Li^+$, the isotherm exhibits a plateau at ca. 5 mN·m$^{-1}$. It resembles the LE/LC phase coexistence region of double-chain phospholipids. However, isotherm measurements show that this plateau rather corresponds to a 2D gas-condensed coexistence (see below). For other alkali metal cations the plateau of that phase transition is expected to be much more extended and hardly observable since the equilibrium 2D gas pressure is much smaller. In the condensed phase region (below 30 Å$^2$·molecule$^{-1}$), the isotherms are also dissimilar. Isotherms for $Rb^+$ and $Cs^+$ have in contrast to others a shoulder at higher pressure, which is usually an indicator of a weak first-order phase transition. The shoulder (indicated with arrow in Figure 1a) is more

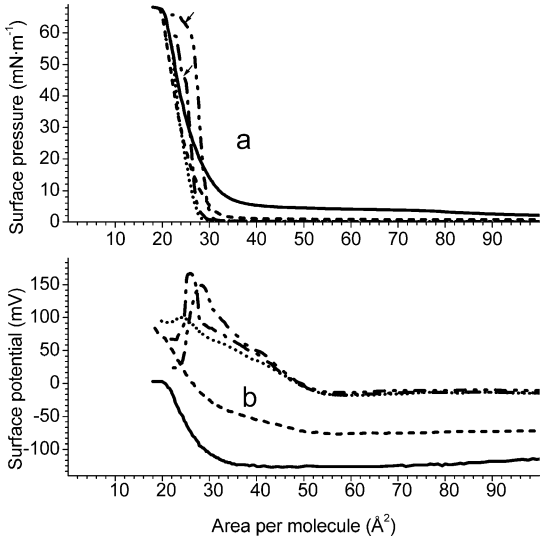


**Figure 1.** Pressure−area (a) and potential−area (b) isotherms of BS monolayers on subphases containing 10 mM of alkali metal chlorides: Li (solid lines); Na (dashed); K (dotted); Rb (dashed−dotted); Cs (dashed−dotted−dotted). Shoulders at pressure−area isotherms (a) are marked with arrows (see text).

pronounced for $Rb^+$ than for $Cs^+$. The maximum slope (elasticity modulus) increases monotonically (with atomic number) from $Li^+$ to $Cs^+$. The area/molecule at a given surface pressure above 40 mN·m$^{-1}$ decreases monotonically from $Cs^+$ to $Na^+$. Only $Li^+$ does not follow this trend.

The observed differences in surface pressure isotherms are assumed to result from different composition/structure of EDL. This is clearly observable in surface potential isotherms (Figure 1b), which differ dramatically. The surface potential of condensed BS monolayers (30 Å$^2$·molecule$^{-1}$) on subphases containing different alkali metal chlorides with the same concentration (10 mM) increases monotonically from $Li^+$ to $Cs^+$ by 200−250 mV. The same order was earlier reported for subphases containing 0.1 mM of alkali metal chlorides.[6] One more feature to be mentioned is the quite unusual sharp maximum in the surface potential plots for $Rb^+$ and $Cs^+$, corresponding to the shoulder in the pressure−area isotherms. This is further evidence of a phase transition, probably associated with charge rearrangement in the monolayer and/or EDL. A possible mechanism could be the penetration of small poorly hydrated counterions into the headgroup region, reducing the EDL potential significantly, with subsequent squeezing out when the packing density of the amphiphiles increases.

If one takes into account that at the same packing density conformation and tilt of monolayer molecules have to be similar, the dipole term of the surface potential is expected to be similar too. In such a case, the difference in surface potential for BS monolayers with different counterions at the same area/molecule results mainly from the difference in potentials of the EDL.[25] It is worth noting that the experimentally observed variation of the surface potential of 200−250 mV is of the same order as the theoretical estimate of the EDL potential for a given charge density and a 10 mM concentration of 1−1-electrolyte. Thus, experimental observations for BS monolayers in the presence of different alkali metal cations contradict strongly the GC model since the EDL potential depends significantly on the type of univalent counterions. The EDL potential's absolute value increases with increasing hydrated counterion size suggesting that packing density limitations play a certain role in EDL formation. Large hydrated counterions (e.g. $Li^+$) require more space than small ones (e.g. $Cs^+$) resulting in thicker EDL with higher electric potential and electrostatic energy.

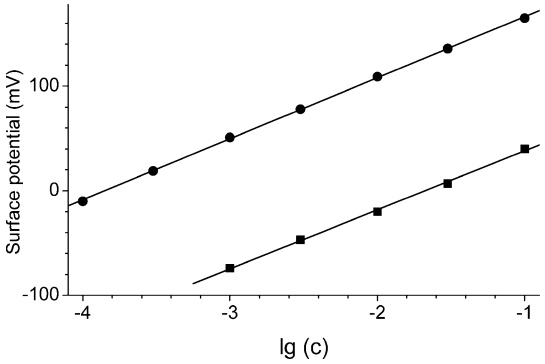


**Figure 2.** Surface potential of BS monolayers (at 25 Å$^2$·molecule$^{-1}$) as a function of electrolyte concentration in the subphase (mole·dm$^{-3}$) containing KCl (●) or LiCl (■). Linear fit: solid lines (slope 58 and 56 mV/decade for KCl and LiCl, respectively).

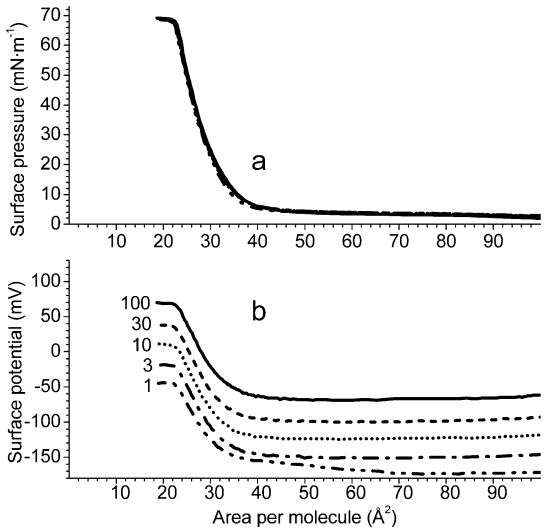


**Figure 3.** Pressure−area (a) and potential−area (b) isotherms of BS monolayers on subphases containing different concentrations of LiCl. Concentrations (in mM) are indicated in plot b; in plot a the curves are overlapping.

At the same time, semilogarithmic plots of monolayer surface potential versus electrolyte concentration (Figure 2) demonstrate precisely the "theoretical slope" for $Li^+$ and $K^+$. Original isotherms are presented in Figure 3 ($Li^+$) and Figure 4 ($K^+$). It is worth noting that the electrolyte concentration (in the range of 0.1−100 mM) has practically no effect on the pressure−area isotherms in both cases. These two facts are closely related with each other. Since the shape of pressure−area isotherms is the same for different electrolyte concentrations, molecular conformation and therefore the dipole term of the surface potential are certainly the same too. Hence, the "theoretical slope" belongs to the EDL potential and is evidence of constant counterion concentration in the vicinity of the monolayer. On the other hand, constant composition of the subphase domain, which is in direct contact with the headgroups, results in the same conformation and packing of monolayer molecules, i.e., similar pressure−area isotherms. Thus, the BS monolayer responding to changes in the electrolyte concentration is in a strict agreement with the GC model.

One more interesting fact is the approximate constant value of the measured surface potential within the gas-condensed coexistence region, manifesting that the condensed domains avoid the measuring zone under the Kelvin probe.[26] In an earlier

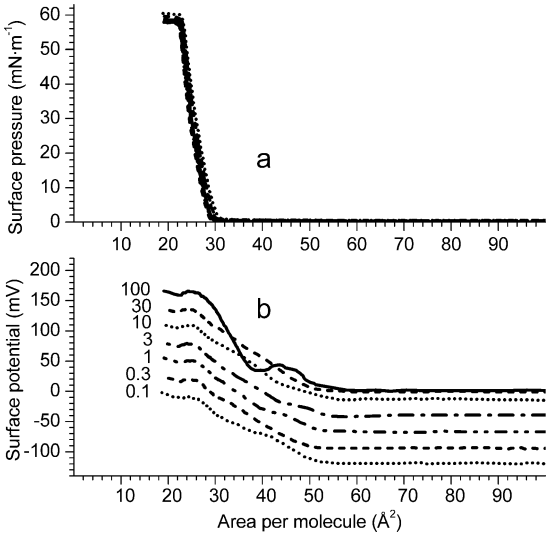


**Figure 4.** Pressure−area (a) and potential−area (b) isotherms of BS monolayers on subphases containing different concentrations of KCl. Concentrations (in mM) are indicated in plot b; in plot a the curves are overlapping.

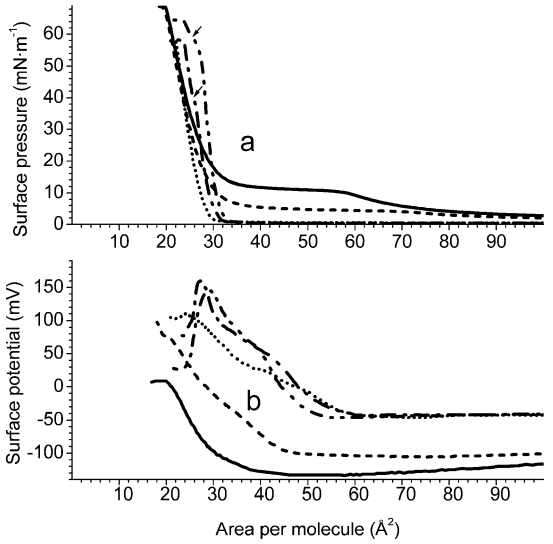


**Figure 5.** Pressure−area (a) and potential−area (b) isotherms of AS monolayers on subphases containing 10 mM of alkali metal chlorides: Li (solid lines); Na (dashed); K (dotted); Rb (dashed−dotted); Cs (dashed−dotted−dotted). Shoulders at pressure−area isotherms (a) are marked with arrows (see text).

study with ionizing electrode such behavior was not observed.[6] The smaller range of the surface potential variation both with the type of alkali metal cation and electrolyte concentration found in a previous study[6] possibly results from traces of divalent cations in their double-distilled water.

Monolayers of arachidyl sulfate (AS) with a hydrocarbon chain two atoms shorter than BS demonstrate very similar effects of alkali metal counterions on the monolayer behavior (Figure 5). In the condensed region, both surface pressure and surface potential isotherms are hardly distinguishable from those of BS monolayers on the same subphases. Due to reduced van der Waals attraction, the gas-condensed coexistence pressure is higher than for BS and the plateau in Figure 5a is observable both for $Li^+$ and $Na^+$. It is remarkable that the AS monolayer on $Li^+$ and $Na^+$ containing subphases remains in the gas state (nonideal) up to very high packing densities (~60 Å$^2$·molecule$^{-1}$). The smooth decrease of the surface pressure with increasing molecular area up to 900 Å$^2$ (data not shown) supports clearly

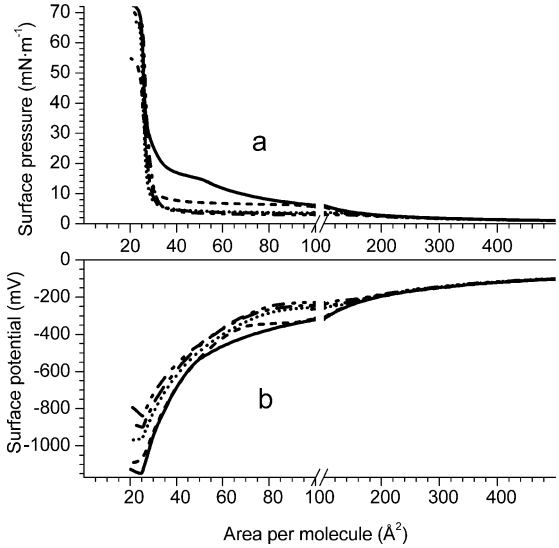


**Figure 6.** Pressure−area (a) and potential−area (b) isotherms of PFMA monolayers on subphases containing 10 mM of alkali metal chlorides: Li (solid lines); Na (dashed); K (dotted); Rb (dashed−dotted); Cs (dashed−dotted−dotted). The horizontal axis is broken to show the highly expanded state of the monolayer.

the gas state of the monolayer at surface pressures below the plateau. Additional experiments with AS monolayers demonstrated that size and charge of electrolyte anions have practically no effect on its behavior in accordance with the classical concept. Possible effects of traces of highly charged cations were excluded in special experiments with the addition of 0.1 mM EDTA and pH adjusted to ca. 9. These experiments show the same monolayer behavior and confirm also the fully ionized state of the monolayer in other experiments.

To ensure that the strong counterion size effect is not inherent to only a particular type of monolayer headgroups, highly negatively charged monolayers of perfluorinated myristic acid (PFMA) were examined. Surface pressure−area isotherms of PFMA on subphases containing different alkali metal cations (Figure 6a) differ markedly in the region between 30 and 200 Å$^2$/molecule. The isotherms exhibit the plateau of 2D gas-condensed coexistence at 15 mN·m$^{-1}$ for $Li^+$, at 7 mN·m$^{-1}$ for $Na^+$, and in the range of 3−4 mN·m$^{-1}$ for the other cations. Upon further expansion, the PFMA monolayer demonstrates typical 2D gaslike behavior, which is independent of the type of alkali metal counterion. In the condensed region (below 30 Å$^2$/molecule) surface pressure isotherms look also very similar. It is worth noting that in this region monolayers exhibit very high 2D viscosity—the Wilhelmy plate moves and tilts from a vertical position with the barrier movement and does not return after compression stops. Although in such a case the shape of isotherms strongly depends on the trough geometry and should be interpreted with precaution, it is unlikely that the amphiphile conformation in the condensed state depends on the type of the counterion.

Surface potential isotherms of PFMA monolayer on subphases with different alkali metal cations (Figure 6b) show negative values, as usually observed for amphiphiles with perfluorocarbon chain.[27] For ionized PFMA, additional negative contribution of the EDL results in extremely high negative surface potential values up to −1100 mV. Additional test experiments with EDTA at pH > 10 exclude effects of traces of highly charged cations and incomplete ionization of the PFMA monolayer. The absolute value of the surface potential of condensed PFMA monolayers (below 30 Å$^2$·molecule$^{-1}$) on subphases with different alkali metal chlorides decreases monotonically from

$Li^+$ to $Cs^+$ by 200−300 mV. Since the dipole term of surface potential, which depends on the amphiphile conformation, does not change significantly, this variation is mainly attributable to changes in the EDL potential. Thus, EDL potential in the case of PFMA monolayer behaves exactly in the same manner as in the case of BS and AS monolayers, which are very dissimilar to PFMA, except for their high negative charge densities. This result suggests that counterion size effects on the EDL potential are rather a general phenomenon for highly charged monolayers and not a result of a particular chemical structure of an amphiphile.

The relative contribution of the EDL to the surface potential of a homogeneously charged monolayer increases with its expansion since the dipole contribution decreases linearly with decreasing packing density, whereas the absolute value of the EDL potential decreases logarithmically. Thus, the absence of counterion size effect on the surface potential of a highly expanded PFMA monolayer in the 2D-gas state indicates the absence of counterion effect on the EDL potential at low surface charge density. The latter is just what one expects in the absence of packing density limitations for counterions.

It is worth noting that in the coexistence region of a 2D-gas and a condensed monolayer (the region 30−150 $Å^2 \cdot molecule^{-1}$ in Figure 6) the interpretation of the surface potential should be avoided, though such interpretation frequently occurs in the literature.[25,28] Since the monolayer is not homogeneous, the measured values strongly depend on particular experimental conditions and are frequently poorly reproducible.[26]

The role of the monolayer surface charge density was specially examined using double-chain amphiphiles as dihexadecyl phosphate (DHDP) and 1,2-dioleoylphosphatidylglycerol (DOPG). DHDP has two saturated C16 hydrocarbon chains and a single-charged headgroup. At low surface pressures, it forms on water a rectangular lattice with chains tilted in the nearest-neighbor (NN) direction. Around 10 $mN \cdot m^{-1}$, the $L_2$ phase transforms into the LS phase[29] on compression. At 20 $mN \cdot m^{-1}$, DHDP occupies a molecular area of 40 $Å^2$.[30] Accordingly, the charge density for condensed DHDP monolayers is roughly one and a half times smaller than that of BS, AS, and PFMA. Having two unsaturated chains and a relatively large headgroup, DOPG forms a liquid-expanded monolayer with an even lower charge density.

Since the phosphate headgroup of DHDP is moderately acidic and suspected of complexation with multivalent cations, all experiments were performed at pH of ca. 10 in the presence of 0.1 mM of EDTA. Surface pressure and surface potential isotherms in the presence of different alkali metal cations are given in Figure 7 and show a rather small influence of the counterion type on the monolayer behavior. Maximum variation of the surface potential is 40−50 mV only. The condensed DHDP monolayer has a very high rigidity, which certainly promotes the formation of holes and possibly collapsed domains. Annealing of defects through 2D evaporation−condensation is ineffective due to immeasurably low 2D-gas pressure, in contrast with PFMA where such a mechanism has to be highly effective. Poor homogeneity of the condensed DHDP monolayer seems to be a reason of reduced reproducibility of surface pressure and surface potential isotherms. Therefore, no further details of alkali metal counterion effects on the DHDP monolayer can be extracted from Figure 7 in a reliable manner. It is worth noting that one of surface potential plots in Figure 7b exhibits oscillations (similar behavior is observable in Figure 4b). Such irregular behavior is inherent to gas-condensed coexistence region of monolayers. The effect results from macroscopic redistribution of condensed domains, and its magnitude depends on variety of factors: particular experimental setup, 2D-gas surface pressure, trace impurities etc.[26]

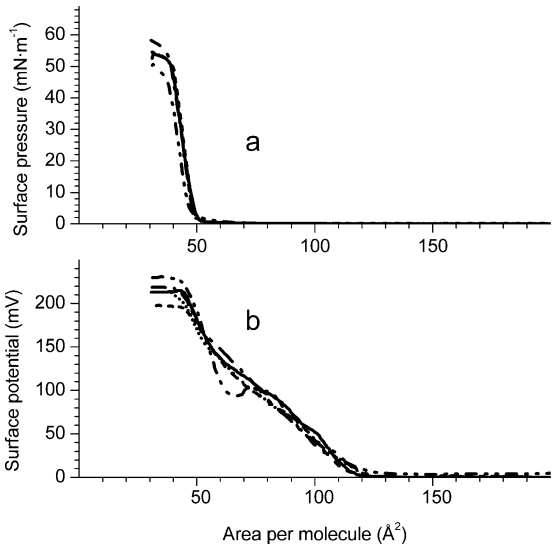


**Figure 7.** Pressure−area (a) and potential−area (b) isotherms of DHDP monolayers on subphases containing 10 mM of alkali metal chlorides: Li (solid lines); Na (dashed); K (dotted); Rb (dashed−dotted); Cs (dashed−dotted−dotted). If one takes into account reduced reproducibility of isotherms for DHDP (see text), the difference between curves in plot a is not significant.

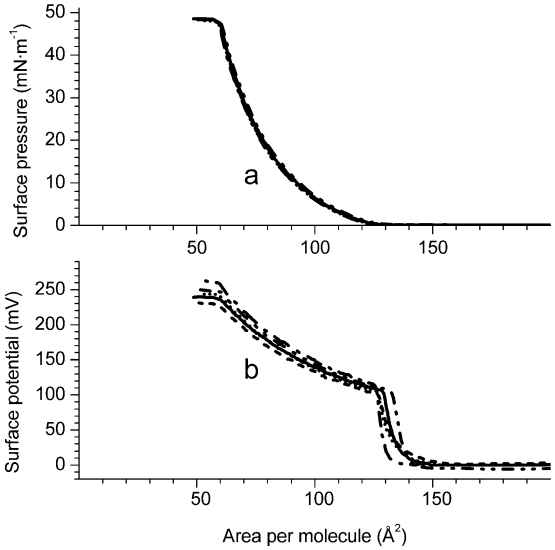


**Figure 8.** Pressure−area (a) and potential−area (b) isotherms of DOPG monolayers on subphases containing 10 mM of alkali metal chlorides: Li (solid lines); Na (dashed); K (dotted); Rb (dashed−dotted); Cs (dashed−dotted−dotted). In both plots the difference between curves is close to the experimental accuracy limit (see text).

In contrast to DHDP, the DOPG monolayer is fluid, which is favorable for high reproducibility of the surface pressure and surface potential isotherms. It was extensively studied in the literature and shown to be fully ionized at pH 5−6 with millimolar salt concentration in the subphase.[18] Surface pressure and surface potential isotherms of DOPG monolayers in the presence of different alkali metal cations (Figure 8) demonstrate practically no influence of counterion type on the monolayer behavior. Maximum variation of the surface potential is about 20 mV. This is rather close to the accuracy limit of the experimental setup and procedures. The same is valid for changes in the pressure−area isotherms also. Thus, the DOPG monolayer with relatively low surface charge density (0.13−

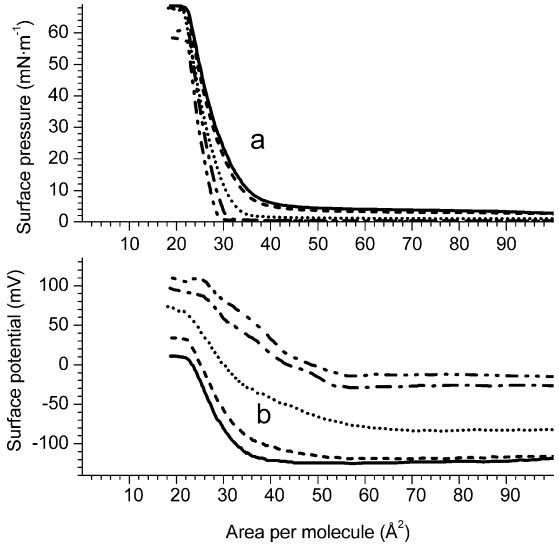


**Figure 9.** Pressure−area (a) and potential−area (b) isotherms of BS monolayers on subphases containing LICl/KCl mixtures with a different fraction of KCl: 0% (solid lines); 1% (dashed); 10% (dotted); 50% (dashed−dotted); 100% (dashed−dotted-dotted). The total concentration of alkali metal chlorides is 10 mM in all cases.

0.27 C·m$^{-2}$ depending on compression) behaves in a good agreement with the GC model of the EDL. Besides the "theoretical slope" of a semilogarithmic plot of monolayer surface potential versus electrolyte concentration,[18] there is practically no effect of counterion size. Additional experiments (data not shown) with fully ionized monolayers of 1,2-dimyristoylphosphatidylserine (DMPS) and 1,2-dipalmitoylphosphatidylglycerol (DPPG)[31] suggest that the negligible effect of alkali metal counterions is likely a common property of negatively charged double-chain phospholipids.

Since the size of counterions affects the electrostatic energy of EDL for highly charged monolayers due to packing density limitations, the free energy of the total system (monolayer + subphase) must be dependent on the counterion size. Therefore, in the presence of two counterions with the same charge but different size, preferential participation of the smaller one in the EDL formation is favorable in terms of free energy. To test this assumption, the BS monolayer was examined on subphases containing two alkali metal cations with distinctly different sizes at different ion ratios with a constant total concentration. Surface pressure and surface potential isotherms of BS monolayers on subphases containing $Li^+$ and $K^+$ are shown in Figure 9. Both isotherms change monotonically with increasing content of $K^+$ in the mixture. At the same time, any particular parameter of both isotherms (gas-condensed coexistence pressure, area at a given pressure, pressure at a given area, surface potential at a given area, etc.) depends in a highly nonlinear way on the $K^+$ molar fraction (data not shown). For the case of $Li^+/Cs^+$ mixtures, the behavior of BS isotherms is generally the same (data not shown). Plots of BS monolayer surface potential versus molar fraction of the smaller cation for $Li^+/K^+$ and $Li^+/Cs^+$ systems are presented in Figure 10. Such behavior suggests that the molar fraction of $K^+$ or $Cs^+$ ions in the EDL is larger than in the bulk phase; i.e., the smaller cations participate preferentially in the EDL formation.

The integral amount of $Cs^+$ in the EDL of BS monolayers was independently determined by means of the X-ray reflectivity technique. BS forms on subphases containing $Li^+$ or $Cs^+$ ions the orthorhombic $L_2$ phase. At 20 mN·m$^{-1}$, the in-plane area on $Li^+$ amounts to 27.5 Å$^2$, whereupon the molecules are strongly tilted by 45° from the surface normal and have a cross-

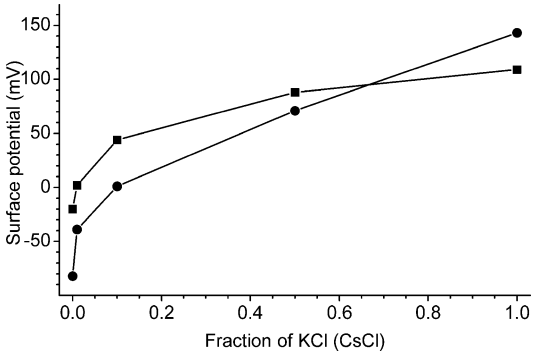


**Figure 10.** Surface potential of BS monolayers on subphases containing mixtures of alkali metal chlorides as a function of the smaller cation fraction: LiCl/KCl (■) mixtures at 25 Å$^2$/molecule; LiCl/CsCl (●) mixtures at 30 Å$^2$·molecule$^{-1}$. The lines are only to guide the eye. The total electrolyte concentration is 10 mM in all cases.

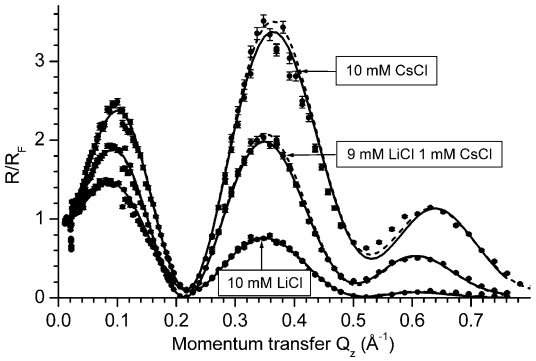


**Figure 11.** X-ray reflectivity plots for BS monolayers on subphases containing LiCl, CsCl, and their mixture at $\pi = 25$ mN·m$^{-1}$. The experimental data are plotted with error bars. The lines (solid and dashed) for each data set present the results of two best fittings. Reflectivity is normalized to Fresnel reflectivity of a pure water surface.

sectional area of 19.6 Å$^2$. The in-plane area on a subphase containing $Cs^+$ is 28.5 Å$^2$, i.e., very similar. The packing is slightly tighter (cross-sectional area of 19.2 Å$^2$), and the molecules are more tilted (48°).

The total number of electrons (parameter responsible for X-ray scattering ability)[32] of a $Cs^+$ cation is comparable with the total number of electrons in the BS headgroup (54 and 48, respectively). Therefore, the integral content of $Cs^+$ in the EDL can be derived from reflectivity data with sufficient accuracy. On the contrary, $Li^+$ with only 3 electrons is practically "invisible" with the X-ray reflectivity technique. Normalized reflectivity data for BS monolayers on subphases with different content of $Cs^+$ at 20 mN·m$^{-1}$ (corresponding to ca. 28 Å$^2$·molecule$^{-1}$) together with the corresponding fits are presented in Figure 11. As it was expected from above considerations, the effect of $Cs^+$ on reflectivity plots is pronounced. The quality of the fits to the experimental data with a 3-layer model (hydrocarbon tails, headgroups, and counterions layer) is not perfect. Nevertheless, profiles of total electron density (Figure 12) reconstructed from slab parameters (electron density, thickness, and roughness) look sufficiently reasonable. Integration of these profiles reveals 50−60% of $Cs^+$ in the EDL compared with 10% $Cs^+$ in the subphase. At this stage, data for 100% $Li^+$ and 100% $Cs^+$ in the subphase were used as calibration references, representing 0 and 100% content of $Cs^+$ in the EDL accordingly. It is worth noting that the qualitative determination of X-ray contrast ions in the vicinity of monolayer headgroups from X-ray reflectivity data does not necessarily require the use of such references.[33,34] Nevertheless, the possibility of independent calibration allows the use of simple "slab

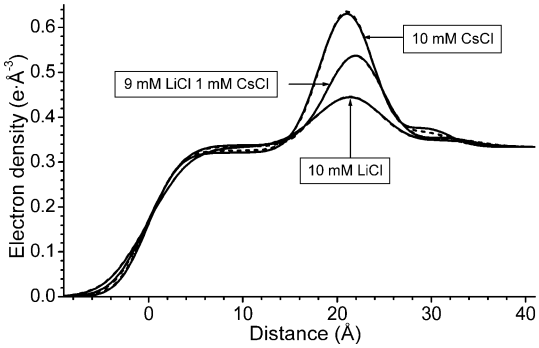


**Figure 12.** Reconstructed electron density profiles for BS monolayers at subphases containing LiCl, CsCl, and their mixture. For each profile, two lines (solid and dashed) correspond to the two best fits presented in Figure 11.

models" and substantially reduces requirements to experimental data quality as well.

Gouy−Chapman theory provides analytical expressions for the potential and ion concentrations in the EDL only for the case of single "symmetric" (1−1, 2−2, etc.) electrolytes. For "asymmetric" electrolytes or mixtures of different electrolytes only the first integration of Poisson−Boltzmann differential equation can be done analytically. The result is known as the Graham equation:[35]

$$\sigma^2 = 2\epsilon\epsilon_0 kT\sum_i n_i(\exp(-z_i e\phi/kT) - 1)$$

(Here $n_i$ and $z_i$ are numeric concentrations and charges for all ions present in the solution).

Analysis of this equation for the case of $\phi \gg kT/e$ reveals two well-known patterns of the GC model: (1) The role of co-ions is negligible. (2) In the presence of different counterions, the effect of the higher charged one is predominant. In other words, an EDL with high potential consists mainly of counterions with the maximum charge. The absence of co-ions in the EDL and therefore their negligible role is evident. However, the situation is not the same for counterions with a different charge, bearing in mind packing density limitations. Indeed, an EDL constructed of small univalent counterions can appear thinner than one constructed of large divalent ones. Since a thinner EDL has less electrostatic potential and energy, small univalent counterions can be competitive with large divalent ones if the surface charge density is high enough for strong packing density limitations to occur.

This assumption was tested experimentally with BS monolayers on subphases containing divalent $Mg^{2+}$ cations (very large in hydrated state) and monovalent alkali metal cations with different size. Corresponding surface pressure and surface potential isotherms are presented in Figure 13. In the presence of only $MgCl_2$ in the subphase, the BS surface pressure isotherm is more expanded compared to most of the alkali metal cations (cf. Figure 1). Moreover, the surface potential of the condensed monolayer is as low as in the case of $Li^+$. Both observations are in agreement with the fact that the size of $Mg^{2+}$ in the hydrated state is very large, even larger than that of $Li^+$ (radii of 4.28 and 3.82 Å, respectively).[22] Similar surface potentials for $Mg^{2+}$ and $Li^+$ together with similar surface pressure isotherms (i.e. similar molecular packing) suggest that the EDL potential is roughly the same for these particular divalent and univalent counterions. This finding contradicts the GC theory that states the EDL potential of univalent counterions has to be ca. 110 mV more negative for the given concentration and surface charge density. The addition of 5 mM of $Li^+$ to 5 mM

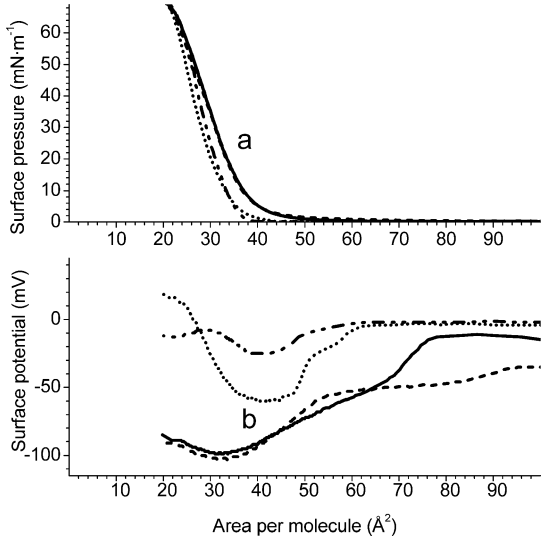


**Figure 13.** Pressure−area (a) and potential−area (b) isotherms of BS monolayer on subphases containing $MgCl_2$ with and without addition of alkali metal chlorides: $MgCl_2$ alone (solid lines); $MgCl_2$ + LiCl (dashed); $MgCl_2$ + KCl (dotted); $MgCl_2$ + CsCl (dashed−dotted−dotted). The concentration of each chloride is 5 mM.

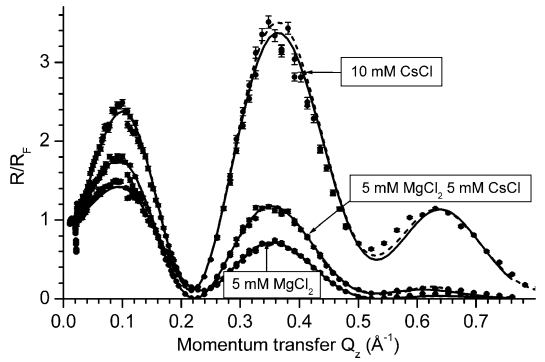


**Figure 14.** X-ray reflectivity plots for BS monolayers at subphases containing $MgCl_2$, CsCl, and their mixture at $\pi$ = 25 mN·m$^{-1}$. Experimental data are plotted with error bars. The lines (solid and dashed) for each data set are the results of two best fittings. Reflectivity is normalized to Fresnel reflectivity of a pure water surface.

of $Mg^{2+}$ has absolutely no effect on both BS isotherms. This is in accordance with Graham equation, i.e., with the GC model—monovalent $Li^+$ is noncompetitive with divalent $Mg^{2+}$. Though present in bulk solution in same concentration as $Mg^{2+}$, it is practically absent in the EDL and certainly does not affect the monolayer properties.

On the contrary, addition of 5 mM of small $K^+$ or $Cs^+$ cations (3.31 and 3.29 Å accordingly)[22] results in significant decrease of surface potential and condensation of BS monolayer, suggesting that these univalent cations are present in EDL to a noticeable extent. Thus, for the case of highly charged BS monolayer small univalent cations are competing successfully with large divalent $Mg^{2+}$ for participation in EDL.

Further confirmation of such "non-Gouy−Chapman" behavior was obtained from X-ray reflectivity experiments utilizing the strong difference in X-ray contrast between $Cs^+$ and $Mg^{2+}$. Reflectivity data and results of their fitting with a 3-layer "slab model" are presented in Figure 14. The effect of 5 mM $Cs^+$ added to the subphase containing the same concentration of $Mg^{2+}$ on reflectivity plots is far outside of possible experimental uncertainty. Integration of total electron density profiles (Figure 15) yields a value of 40−50% for the Cs ions contribution to the total charge of cations in the EDL (close to the negative

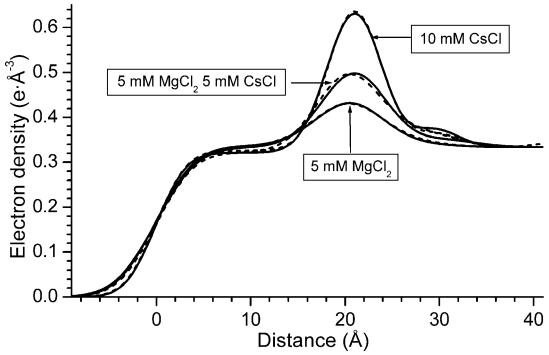


**Figure 15.** Reconstructed electron density profiles for BS monolayers at subphases containing $MgCl_2$, CsCl, and their mixture. For each profile two lines (solid and dashed) correspond to the two best fits presented in Figure 14.

charge of the headgroups). This contribution corresponds to a $Cs^+/Mg^{2+}$ratio in the range 1.3−2. For comparison, application of the GC model gives a ratio of ca. 0.04 (estimated from numeric integration of the Poisson−Boltzmann equation for appropriate charge density and electrolyte concentrations).

## Conclusion

Deviations from the GC model due to finite size of counterions (packing density limitation) were tested for negatively charged Langmuir monolayers with different charge densities. Special attention was paid to minimum complexing ability of monolayer headgroups with respect to cations and full ionization of headgroups at experimental conditions, providing a known and stable negative charge density of each monolayer.

For monolayers with the largest charge density (0.64 $C \cdot m^{-2}$), the surface potential increases monotonically from $Li^+$ to $Cs^+$ by 200−250 mV. This effect is practically the same for different monolayers with similar values of negative charge density. Therefore, it is likely a general phenomenon and not inherent to some particular monolayer or headgroup. With plausible assumption that the dipole term of the surface potential is approximately constant for a given monolayer packing density, the observed change in the surface potential results mainly from an increase (by absolute value) in the negative EDL potential with increasing size of hydrated counterions. Such behavior is in strong contradiction with the GC model, since 200−250 mV is roughly equal to the theoretically estimated EDL potential for the appropriate charge density and electrolyte concentration. At the same time, semilogarithmic plots of monolayer surface potential versus electrolyte concentration demonstrate precisely the "theoretical slope" predicted by the GC model.

As one could expect, this kind of discrepancy with the classical model rapidly vanishes with decreasing monolayer charge density. For the DHDP monolayer with charge density of ca. 0.4 $C \cdot m^{-2}$, it is already 5 times smaller. For the biologically relevant case of negatively charged phospholipids with a charge density of 0.1−0.3 $C \cdot m^{-2}$, this effect is hardly observable for alkali metal cations within the usual accuracy of surface potential experiments. Again, this is unlikely related to a particular type of chemical group, since it is also observed for highly expanded PFMA monolayers.

Since the size of counterions affects the EDL thickness, the electrostatic term of the free energy of the total system (monolayer + subphase) appears to be dependent on counterion size for highly charged monolayers. Therefore, in the presence of two counterions, preferential participation of the smaller one in the EDL formation is favorable in terms of free energy. Direct determination of the relative amount of $Cs^+$ in the EDL of BS monolayers from X-ray reflectivity data gives 50−60% of $Cs^+$ in the EDL in the presence of only 10% of $Cs^+$ in the subphase.

Small univalent $Cs^+$ cations can even compete with large divalent $Mg^{2+}$ ions. X-ray reflectivity data for BS monolayers in the presence of equal concentrations of $Cs^+$ and $Mg^{2+}$ in the subphase yield a $Cs^+/Mg^{2+}$ ratio in the range 1.3−2. This finding is in dramatic contradiction with the GC model, which gives only 0.04 for such a ratio. At the same time, large $Li^+$ cations behave in accordance with the GC model: they are unable to compete with divalent $Mg^{2+}$.

Our experimental data show clearly the ion size effect on the EDL formation at highly negatively charged surfaces. In a further publication, we will present systematic experimental study of the counterion size effect for positively charged monolayers.

**Acknowledgment.** V.L.S. thanks the RFBR (Project 05-03-32580) for financial support. This work was supported by the DFG (Grant MO283/35). We thank HASYLAB at DESY, Hamburg, Germany, for beam time and providing excellent facilities and support. The authors are grateful to Prof. O. Shibata for providing purified PFMA and to Dr. O. V. Konovalov for his invaluable help in fitting the X-ray reflectivity data.

## References and Notes

(1) Goddard, E. D.; Kao, O.; Kung, H. C. *J. Colloid Interface Sci.* **1968**, *24*, 297−309.

(2) Dreher, K. D.; Wilson, J. E. *J. Colloid Interface Sci.* **1970**, *32*, 248−255.

(3) Harada, M.; Okada T. *Langmuir* **2004**, *20*, 30−32.

(4) Gilanyi, T.; Varga, I.; Meszaros, R. *Phys. Chem. Chem. Phys.* **2004**, *6*, 4338−4346.

(5) Ahuja, R. C.; Caruso, P. L.; Möbius, D. *Thin Solid Films* **1994**, *242*, 195−200.

(6) Goddard, E. D.; Kao, O.; Kung, H. C. *J. Colloid Interface Sci.* **1968**, *27* (4), 616−624.

(7) Benrraou, M.; Bales, B. L.; Zana, R. *J. Phys. Chem. B* **2003**, *107*, 13432−13440.

(8) Ropers, M. H.; Czichocki, G.; Brezesinski, G. *J. Phys. Chem. B* **2003**, *107*, 5281−5288.

(9) Nascimento, D. B.; Rapuano, R.; Lessa, M. M.; Carmona-Ribeiro, A. M. *Langmuir* **1998**, *14*, 7387−7391.

(10) Colic, M.; Franks, G. V.; Fisher, M. L.; Lange, F. F. *Langmuir* **1997**, *13*, 3129−3135.

(11) López-León, T.; Jódar-Reyes, A. B.; Bastos-González, D.; Ortega-Vinuesa, J. L. *J. Phys. Chem. B* **2003**, *107*, 5696−5708.

(12) Jiang, N.; Li, P. X.; Wang, Y. L.; Wang, J. B.; Yan, H. K.; Thomas, R. K. *J. Colloid Interface Sci.* **2005**, *286*, 755−760.

(13) Lonetti, B.; Lo Nostro, P.; Ninham, B. W.; Baglioni, P. *Langmuir* **2005**, *21*, 2242−2249.

(14) Gurau, M. C.; Lim, S. M.; Castellana, E. T.; Albertorio, F.; Kataoka, S.; Cremer, P. S. *J. Am. Chem. Soc.* **2004**, *126*, 10522−10523.

(15) Zemb, Th.; Belloni, L.; Dubois, M.; Aroti, A.; Leontidis, E. *Curr. Opin. Colloid Interface Sci.* **2004**, *9*, 74−80.

(16) Ohki, S.; Sauve, R. *Biochim. Biophys. Acta* **1978**, *511*, 377−387.

(17) Ohki, S.; Sauve, R. *Biochim. Biophys. Acta* **1981**, *645*, 170−176.

(18) Zakharov, S. D.; Rokitskaya, T. I.; Shapovalov, V. L.; Antonenko, Yu. N.; Cramer, W. A. *Proc. Natl. Acad. Sci. U.S.A.* **2002**, *99* (13), 8654−8659.

(19) Gaines, J. L., Jr. *Insoluble monolayers at liquid−gas interfaces*; Interscience Publishers: New York, 1966; p 195.

(20) Jaycock, M. J.; Parfitt, G. D. *Chemistry of Interfaces*; Ellis Horwood: Chichester, U.K., 1981.

(21) Spitzer, J. J. *Langmuir* **2003**, *19*, 7099−7111.

(22) Nightingale, E. R., Jr. *J. Phys. Chem.* **1959**, *68*, 1381−1387.

(23) Jensen, T. R.; Kjaer, K.; Brezesinski, G.; Ruiz-Garcia, J.; Möhwald, H.; Makarova, N. N.; Godovsky, Yu. K. *Macromolecules* **2003**, *36*, 7236−7243.

(24) Samoilenko, I. I.; Konovalov, O. V.; Feigin, L. A.; Shchedrin, B. M.; Yanusova, L. G. *Crystallogr. Rep.* **1999**, *44* (2), 310−318.

(25) Cavalli, A.; Dynarowicz-Latka, P.; Oliveira, O. N., Jr.; Feitosa, E. *Chem. Phys. Lett*. **2001**, *338*, 88−94.

(26) Shapovalov, V. L.; Shub, B. R.; Oliveira, O. N., Jr. *Colloids Surf., A* **2002**, *198*−*200*, 195−206.

(27) Shibata, O.; Yamamoto, S. K.; Lee, S., Sugihara, G. *J. Colloid Interface Sci.* **1996**, *184*, 201−208.

(28) Oliveira, O. N., Jr.; Taylor, D. M.; Morgan, H. *Thin Solid Films* **1992**, *210*−*211*, 76−78.

(29) Kaganer, V. M.; Möhwald, H.; Dutta, P. *Rev. Mod. Phys.* **1999**, *71*, 779−819.

(30) Lehmann, P.; Kurth, D. G.; Brezesinski, G.; Symietz, C. *Chem.*−*Eur. J.* **2001**, *7*, 1646−1651.

(31) Maltseva, E.; Shapovalov, V. L.; Brezesinski, G.; Möhwald, H. *J. Phys. Chem. B* **2006**, *110* (2), 919−926.

(32) Krüger, P.; Schalke, M.; Linderholm, J.; Lösche, M. *Rev. Sci. Instrum.* **2001**, *72*(1), 184−192.

(33) Schalke, M.; Lösche, M. *Adv. Colloid Interface Sci.* **2000**, *88*, 243−274.

(34) Cuvillier, N.; Rondelez, F. *Thin Solid Films* **1998**, *327*−*329*, 19−23.

(35) Graham, D. C. *Chem. Rev.* **1947**, *41*, 441−501.